Lamb-shift calculations for non-Coulomb potentials

K. T. Cheng
University of California, Lawrence Livermore National Laboratory, P.O. Box 808, Livermore, California 94550

W. R. Johnson and J. Sapirstein
Department of Physics, University of Notre Dame, Notre Dame, Indiana 46556

(Received 24 September 1992)

QED effects associated with the electron self-energy and vacuum polarization are calculated in non-Coulomb potentials for atomic states with principal quantum numbers 1 and 2. We consider the Coulomb potential with finite nuclear size incorporated and using the core-Hartree potential, a local version of the Hartree-Fock potential. The calculations are carried out for ions with nuclear charges in the range Z=60–90. For the Coulomb potential with finite nuclear size, substantial discrepancies with an earlier tabulation are found. Radiative corrections are calculated for lithiumlike uranium using the core-Hartree potential and comparison with experiment is made.

PACS number(s): 31.30.Jv, 12.20.Ds, 31.20.Tz

I. INTRODUCTION

The study of the spectra of highly charged ions with more than one electron presents a fundamental challenge to the understanding of the relativistic many-body problem and its proper setting in the framework of quantum electrodynamics (QED). While this problem could be posed for the energy levels of any atomic system, the effects of interest, relativistic and QED corrections, are generally much smaller than the wave-function uncertainties arising from approximations in the solution to the Schrödinger equation. In highly charged ions, however, the QED corrections are enhanced by powers of the nuclear charge Z at the same time that the $1/Z$ expansion [1] allows for a rapidly convergent many-body perturbation-theory (MBPT) solution to the Schrödinger equation. Because of considerable progress in the experimental measurement of the spectra of a number of isoelectronic sequences, a new set of systems in which precision tests of QED can be made is becoming available. The standard tests of QED, from the study of lepton anomalous magnetic moments, the spectra of one-electron atoms, and the spectrum of neutral helium, can now be extended to highly charged ions, which test the theory in intense Coulomb fields.

After closed-shell ions, the simplest many-electron ions are alkali-metal-like, with one valence electron outside a closed shell. Application of MBPT to such ions results in a clear pattern of convergence [2]. When MBPT calculations are compared with experiment, systematic discrepancies result that are identified as QED effects. These discrepancies can be compared to the predictions of QED for the case when the electrons in the core are not present, as this reduces the problem to the well understood one-electron Lamb-shift calculation [3]. The one-loop Lamb shift scales as $Z^4\alpha^3$ a.u., and comes from the evaluation of the Feynman diagrams of Figs. 1(a) and 1(b), which are associated with the electron self-energy and vacuum polarization, respectively. When the one-electron Lamb-shift is included, it is seen that the bulk of the experimentally inferred QED effect is accounted for, but this effect is systematically smaller than the one-electron prediction. This result is intuitively obvious, since the neglected core electrons should act to reduce the effective nuclear charge seen by the valence electron, thereby reducing the one-electron Lamb shift. It is possible to introduce various phenomenological methods of incorporating this effect by interpolating the one-electron Lamb-shift tables [4]. However, a more fundamental approach is to calculate the effect directly from QED. This can be done using S-matrix techniques [5]. These techniques employ the symmetric extension of the Gell-Mann–Low formalism [6] derived by Sucher [7] to express atomic energy levels directly in terms of Feynman diagrams in the Furry representation [8]. For highly charged ions only a limited set of diagrams need be considered because of the $1/Z$ expansion. We illustrate in Fig. 2 representative diagrams involving two-photon exchange. Some of these diagrams can be shown to directly correspond to MBPT, and others are directly connected with the Lamb shift [9]. However, the electron propagators in these diagrams are not necessarily Dirac-Coulomb propagators, but are rather propagators in the local potential used to define the Furry representation. This potential can be chosen to be the Coulomb potential of a point nucleus, in which case the diagrams of Fig. 1 have already been evaluated and attention can be focused on the diagrams of

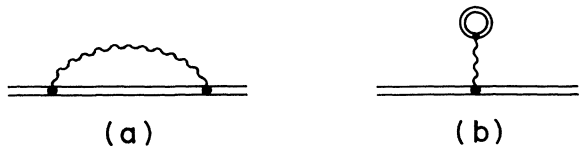

FIG. 1. (a) Electron self-energy diagram. (b) Vacuum polarization diagram.

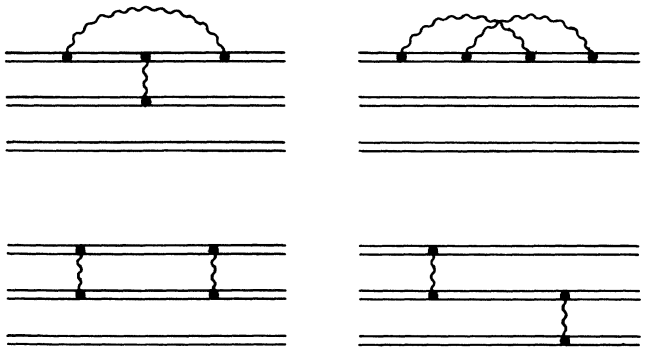

FIG. 2. Representative two-photon diagrams.

Fig. 2. However, if one is interested in calculating radiative corrections in a many-electron atom, even at high Z the Coulomb potential is not an appropriate starting point. In addition, if one wants to account for the effect of the finite size of the nucleus on radiative corrections, a non-Coulomb potential should be used. Thus there is considerable interest in evaluating the Lamb shift in non-Coulomb potentials that incorporate this additional physics. The purpose of this paper is to present such calculations. We will see that when these calculations are combined with MBPT for lithiumlike uranium, agreement with experiment at the few tenths of an eV level is found. However, the QED parts of the diagrams of Fig. 2 can contribute at the same level, and must also be calculated before it can be claimed that this comparison is testing QED: they will be discussed in the conclusion. It should be emphasized that this paper is the first step in a two-part process of evaluating the one-loop Lamb shift in non-Coulomb potentials and then calculating in the same non-Coulomb potentials the QED part of the diagrams of Fig. 2. The plan of the paper is as follows. In Sec. II we describe the non-Coulomb potentials we use. In Sec. III an overview of the self-energy calculation is given, followed in Sec. IV by a detailed description of the present calculation and a set of tables. Finally in Sec. V we compare with other calculations and experiment, and discuss directions of future progress.

II. CHOICE OF NON-COULOMB POTENTIALS

We consider two different non-Coulomb potentials in this paper. The first is appropriate for one-electron ions with the nuclear finite size taken into account. When this finite size is modeled with a uniform charge distribution or a shell of charge, analytic methods can be used to treat the electron Green's function. However, because our approach is purely numerical, we can choose instead the more realistic Fermi distribution, in which

$$\rho(x) = \frac{\rho_0}{1 + e^{(x-c)/a}}, \tag{1}$$

where, following Ref. [10], we choose a=0.523 fm and c so that the root-mean-square radius obeys

$$\langle r^2 \rangle^{1/2} = (0.836A^{1/3} + 0.570) \text{ fm} \tag{2}$$

if the radius was not explicitly measured, and the measured result otherwise.

For the case of one-valence electron ions, we want a local potential that approximates the Hartree-Fock potential, which would significantly complicate the calculations because of its nonlocality. A local potential that has elements of self-consistency and has the physical long-range behavior appropriate to alkali systems is the *core-Hartree* potential, defined by

$$V_{\rm CH}(r) = V_{\rm nuc}(r) + \sum_a (2j_a + 1) v_0(a, a; r) \tag{3}$$

where

$$v_0(a, a; r) \equiv \int dr' \frac{1}{r_>} [g_a^2(r') + f_a^2(r')]. \tag{4}$$

Here a refers to a state in the core and g_a and f_a are the upper and lower components of the associated Dirac spinors. These states a are determined self-consistently in the potential $V_{\rm CH}(r)$. If there are N electrons in the core, the long-range behavior of this potential will be $-(Z-N)/r$, so that high-Rydberg valence-electron states will see the correct potential.

III. ELECTRON SELF-ENERGY CALCULATIONS

The Lamb shift has two distinct contributions, vacuum polarization and electron self-energy. These two effects have been intensively studied for hydrogenic ions. Vacuum polarization is comparatively simple, and has been treated by numerous authors [11]. The self-energy is considerably more difficult to treat. For low Z, a perturbative expansion in $(Z\alpha)$ has been carried out [12] to order $Z^6\alpha^5$. For high values of Z, this expansion breaks down, and numerical methods are needed to carry out the calculation nonperturbatively. The original approach to this problem was introduced by Brown, Langer, and Schaefer (BLS) [13] in 1959, and was used to calculate the $1s$ energy shift of mercury by Brown and Mayers [14]. Analytic and numerical errors in these papers were later corrected in Ref. [15]. For brevity we will refer to this calculational method as the BLS method in the following. This method was used to calculate finite-nuclear-size effects in Refs. [16] and [17]. A somewhat different method of calculation was employed by Mohr [3] for the very-high accuracy evaluation of the self-energy for the Coulomb case for $n = 1$ and 2 states, and more recently by Kim and Mohr [18] for $n = 3$, 4, and 5 states. In a recent paper [19] we reported an extension of the BLS method to $n = 2$, 3, and 4 states. This extension consisted of including substantially more partial waves than in earlier work and controlling the leading $1/l^2$ behavior of the partial wave expansion. An important improvement of the method has recently been suggested by Snyderman [20] and numerically implemented by Blundell and Snyderman [21], who found that it leads to a rapidly convergent partial wave expansion. We have modified our approach to incorporate this improvement, and find excellent agreement with the Coulomb results presented in [21] and the non-Coulomb results recently presented by Blundell [22].

The electron self-energy (SE) of a state n is given by

$$\Delta E_n(\mathrm{SE}) = -ie^2 \int d^3r\, d^3r' \int \frac{d^4k}{(2\pi)^4} \frac{e^{i\mathbf{k}\cdot(\mathbf{r}-\mathbf{r}')}}{k^2+i\epsilon} \bar{\psi}_n(\mathbf{r})\gamma_\mu S_F(\mathbf{r},\mathbf{r}';E_n-k_0)\gamma^\mu\psi_n(\mathbf{r}') - \delta m^{(2)} \int d^3r\, \bar{\psi}_n(\mathbf{r})\psi_n(\mathbf{r}), \quad (5)$$

where $\delta m^{(2)}$ is the ultraviolet divergent electron self-mass and the electron propagator in an external potential $V(\mathbf{r})$ satisfies the equation

$$S_F(\mathbf{r},\mathbf{r}';E) = S_F^0(\mathbf{r},\mathbf{r}';E) + \int d^3x S_F^0(\mathbf{r},\mathbf{x};E)\gamma_0 V(\mathbf{x}) S_F^0(\mathbf{x},\mathbf{r}';E) + \int d^3x\, d^3y\, S_F^0(\mathbf{r},\mathbf{x};E)\gamma_0 V(\mathbf{x}) S_F(\mathbf{x},\mathbf{y};E)\gamma_0 V(\mathbf{y}) S_F^0(\mathbf{y},\mathbf{r}';E) \quad (6)$$

with $S_F^0(\mathbf{x},\mathbf{y};E)$ being the free-electron propagator. The ultraviolet divergences of the self-energy are associated with the first two terms of Eq. (6), with the third term giving a finite contribution. We will in the following refer to the first, second, and third terms of Eq. (6) when put in the first term of Eq. (5) as the zero-potential, one-potential, and many-potential terms, respectively. The BLS method involves isolating the zero-potential term. This is done by evaluating the first term in Eq. (5) by explicitly subtracting S_F^0 from S_F in coordinate space, and adding the S_F^0 term, evaluated in momentum space, back in. However, while part of the latter term directly cancels the second term of Eq. (5), an ultraviolet divergence associated with the electron wave-function renormalization constant remains in that term even after that cancellation. This divergence can be expressed as an integral over ω of the form $\int d\omega/\omega$, where this variable is the time component of the d^4k integration after a Wick rotation $k_0 \to i\omega$. When the same Wick rotation is carried out for the term involving the difference of S_F and S_F^0, a canceling $\int d\omega/\omega$ integral results, so that a finite answer is obtained after combining all terms. This is because this difference still contains the one-potential term, which has a divergent vertex renormalization constant that cancels with the wave-function renormalization constant by Ward's identity. This answer, referred to here as the main term, must be combined with the finite part of the S_F^0 term and a term called the pole term coming from the contour shift in the Wick rotation involving the complete or partial encircling of more deeply bound or degenerate states, respectively. By far the most difficult numerical problems of the BLS method arise in the evaluation of the main term. This is because an infinite partial-wave expansion must be carried out to get the integrand as a function of ω, which for high ω behaves as $1/\omega$. After the canceling $1/\omega$ term from the S_F^0 term is included, the high-energy behavior of the integrand falls off more rapidly with ω. However, significant contributions to the Lamb shift come from high values of ω, and the fact that the partial-wave expansion can only be carried out approximately becomes a problem here. That is because the expansion does not become asymptotic at the values of l we were able to control, about $l = 100$, for high values of ω. Therefore it was necessary to introduce fits for the asymptotic ω dependence of the integrand using the relatively low values of ω, on the order of a few electron masses, where we retained control of the calculation. Different fits gave consistent values for the self-energy, but could differ by several thousandths of an atomic unit. At this level of accuracy the BLS method does allow the calculation of the electron self-energy in non-Coulomb fields, but for higher accuracy some new method is needed.

We have chosen for this new method a variation of the method used by Blundell and Snyderman [21]. The basic idea is to evaluate only the many-potential term in coordinate space, using a partial-wave expansion, and to evaluate the one-potential term explicitly in momentum space. This isolation of both the zero-potential and one-potential terms allows the direct cancellation of all ultraviolet divergences at the cost of a more complicated momentum space integration. However, the great advantage of this is the increased convergence of the main term, which now for large l falls as $1/l^3$ rather than $1/l^2$. In addition, the integrand falls more rapidly at high ω, and no cancellation of individually logarithmically divergent terms is required. Blundell and Snyderman chose to evaluate this modified main term using the third term of Eq. (6) directly, representing the free and bound propagators as spectral representations based on finite basis sets constructed from B splines. Here, however, we note that the same result follows from subtracting the one-potential term as well as the zero-potential term from the bound-state propagator. Although the same basic quantity is being evaluated, it should be emphasized that the method of calculation is completely different, and the good agreement between the two methods provides a nontrivial cross-check. Recently a novel approach to the calculation of the self-energy has been proposed [23, 24] in which Eq. (5) is evaluated without any subtractions other than the self-mass counterterm, which is evaluated numerically. When applied to lithiumlike uranium, this method gives good agreement [23] with the the results of Refs. [19, 22] and the present paper.

IV. CALCULATION

The calculation proceeds in detail as follows. For purposes of illustration, the individual terms of a particu-

lar calculation, the $2s_{1/2}$ and $2p_{1/2}$ self-energies of lithiumlike uranium in the core-Hartree potential, are given in Table I. We first consider the zero- and one-potential terms that were subtracted from the first term of Eq. (5). They are evaluated in momentum space after being made finite with dimensional regularization. The zero-potential term has two kinds of ultraviolet divergence, and can be written

$$\Delta E_n^{0\text{-pot}} = \delta m^{(2)} \int d^3p\, \bar{\psi}_n(\mathbf{p})\psi_n(\mathbf{p}) - \frac{\alpha}{2\pi}\left(\frac{C}{\epsilon}+1\right)\int d^3p\, \bar{\psi}_n(\mathbf{p})(\not{p}-m)\psi_n(\mathbf{p})$$
$$-\frac{\alpha}{2\pi}\int d^3p \int_0^1 dx \frac{1-\epsilon_n^2+\mathbf{p}^2/m^2}{1-\epsilon_n^2(1-x)+(1-x)\mathbf{p}^2/m^2}\bar{\psi}_n(\mathbf{p})[2m-\not{p}(1-x/2)]\psi_n(\mathbf{p}). \tag{7}$$

The constant C is

$$C = (4\pi)^{\epsilon/2}\Gamma(1+\epsilon/2), \tag{8}$$

where ϵ is a small positive quantity related to the dimension of space-time n by $n = 4-\epsilon$, and is to be distinguished from the energy of state n in mass units $\varepsilon_n = E_n/m$. The self-mass counterterm is

$$\delta m^{(2)} = \frac{m\alpha}{\pi}\left(\frac{3C}{2\varepsilon}+1\right). \tag{9}$$

The one-potential term can be reduced to

$$\Delta E_n^{1\text{-pot}} = \frac{\alpha}{2\pi}\left(\frac{C}{\varepsilon}-1\right)\int d^3p\, \bar{\psi}_n(\mathbf{p})(\not{p}-m)\psi_n(\mathbf{p})$$
$$+\frac{Z\alpha^2}{4\pi^3}\int_0^1 \rho\, d\rho \int_0^1 dx \int \frac{d^3p d^3p'}{|\mathbf{p}-\mathbf{p}'|^2}\bar{\psi}_n(\mathbf{p})\gamma_0\psi_n(\mathbf{p}')\ln\left(\frac{\Delta}{m^2}\right) + \frac{Z\alpha^2}{8\pi^3}\int_0^1 \rho\, d\rho \int_0^1 dx \int \frac{d^3p\, d^3p'}{|\mathbf{p}-\mathbf{p}'|^2}\frac{N}{\Delta}, \tag{10}$$

where

$$\Delta = \rho^2 E_n^2 - \rho^2|x\mathbf{p}+(1-x)\mathbf{p}'|^2 + \rho(m^2-E_n^2) + \rho x\mathbf{p}^2 + \rho(1-x)\mathbf{p}'^2 \tag{11}$$

and

$$N = -2[m^2+E_n^2(1-\rho)^2]\bar{\psi}_n(\mathbf{p})\gamma_0\psi_n(\mathbf{p}') + 8mE_n(1-\rho)\bar{\psi}_n(\mathbf{p})\psi_n(\mathbf{p}')$$
$$+2E_n(1-\rho)\bar{\psi}_n(\mathbf{p})\boldsymbol{\gamma}\cdot(\mathbf{p}+\mathbf{p}'-2\mathbf{Q})\psi_n(\mathbf{p}') - 2\psi_n^\dagger(\mathbf{p})\boldsymbol{\alpha}\cdot(\mathbf{p}'-\mathbf{Q})\boldsymbol{\alpha}\cdot(\mathbf{p}-\mathbf{Q})\psi_n(\mathbf{p}'), \tag{12}$$

where

$$\mathbf{Q} \equiv \rho[x\mathbf{p}+(1-x)\mathbf{p}']. \tag{13}$$

The zero- and one-potential terms can now be combined with the self-mass counterterm to give an ultraviolet finite result. Thus the zero-potential term that is numerically evaluated, which is denoted as $E^{(0-P)}$, is taken to be Eq. (7) without the δm and C/ε terms, and the one-potential term, denoted as $E^{(1-P)}$, is taken to be Eq. (10) without the C/ε term. While the zero-potential term is relatively simple to evaluate, the multidimensional integration in the one-potential term presents more difficulties, since even after carrying out the ρ integration analytically it is a four-dimensional integral. We evaluated it numerically using Monte Carlo methods [25], as opposed to the Gaussian techniques used in Refs. [21] and [22].

After these subtractions are carried out, we are left with a finite integral we evaluate in coordinate space that we call the modified main term, to distinguish it from the main term in the BLS method. The Wick rotation that takes $k_0 \to i\omega$ passes bound-state poles, however, in exactly the same manner as in that original scheme, since the one-potential term being subtracted has no bound state poles. Thus the pole terms are still given by

$$\Delta E_n^{\text{pole}} = \alpha \sum_{\epsilon_a<\epsilon_n}\int \frac{d^3x\, d^3y}{|\mathbf{x}-\mathbf{y}|}\bar{\psi}_n(\mathbf{x})\gamma_\mu\psi_a(\mathbf{x})\bar{\psi}_a(\mathbf{y})\gamma^\mu\psi_n(\mathbf{y})e^{i(\epsilon_n-\epsilon_a)|\mathbf{x}-\mathbf{y}|}$$
$$+\frac{\alpha}{2}\sum_{\epsilon_a=\epsilon_n}\int \frac{d^3x\, d^3y}{|\mathbf{x}-\mathbf{y}|}\bar{\psi}_n(\mathbf{x})\gamma_\mu\psi_a(\mathbf{x})\bar{\psi}_a(\mathbf{y})\gamma^\mu\psi_n(\mathbf{y}). \tag{14}$$

The second term in the above equation enters only in the Coulomb case where states can be degenerate. We evaluate here only the real part of ΔE_n^{pole}: the imaginary part either describes the decay rate of a one-electron system or else cancels an imaginary part from the Breit interaction for many-electron systems.

The modified main term is evaluated as follows. The bound and free-electron propagators are evaluated nu-

TABLE I. Breakdown of self-energy for the the $2s_{1/2}$ and $2p_{1/2}$ states of lithiumlike uranium: core-Hartree case with finite nuclear size (in a.u.).

Term	$2s_{1/2}$	$2p_{1/2}$	$2p_{1/2} - 2s_{1/2}$
Pole	10.2707	11.8932	1.6225
$E^{0\text{-}P}$	−9.0694	−10.4575	−1.3881
$E^{1\text{-}P}$	6.9313(5)	6.2110(4)	−0.7203(6)
$l = 0$	−6.4389	−1.7112	4.7277
$l = 1$	0.3727	−5.9712	−6.3439
$l = 2$	0.1200	0.2077	0.0877
$l = 3$	0.0495	0.0687	0.0192
$l = 4$	0.0244	0.0296	0.0052
$l = 5$	0.0135	0.0151	0.0016
$l = 6$	0.0081	0.0087	.0006
$l = 7$	0.0052	0.0054	0.0002
$l = 8$	0.0035	0.0036	0.0001
$l = 9$	0.0025	0.0025	0.0000
$l = 10$	0.0018	0.0018	0.0000
$l = 11$	0.0013	0.0013	0.0000
$l = 12$	0.0010	0.0010	0.0000
$l = 13$–∞	0.0056(2)	0.0056(2)	0.0000(1)
Self-energy	2.3029(5)	0.3153(4)	−1.9876(6)
Uehling potential	−0.5783	−0.0961	0.4822

merically in terms of solutions to the Dirac equation regular at the origin and infinity using a 4000-point radial grid, and the main term is evaluated along the lines of the BLS method. This leads to a table of results for given values of ω and l. Next the one-potential term is evaluated for exactly the same values of ω and l and subtracted from the previous table. At this point, because the ω integration is finite, we carry it out with Gaussian integration. It is necessary to take care with this integration at low ω when dealing with the finite-nuclear-size case because a large contribution that is related to the pole terms is present when $\omega \sim \epsilon_n - \epsilon_a$, where a is a state nearly degenerate with n. The large ω region, which was the principal source of numerical difficulty in the BLS method, can be directly integrated over with the present method because low partial waves do not present the same difficulties. Typically we integrated from zero to five electron masses with a large number of Gaussian points (isolating the very small ω region for the finite nucleus case) and then transformed the remaining integral to infinity to a finite region which could be evaluated with a smaller number of Gaussian points. Once the ω integral for fixed values of l was carried out, we found a set of l values that fell for high l as $1/l^3$. The result is dominated by very low l, with the bulk of the contribution coming from $l = 0, 1$, and 2. We have explicitly calculated up to $l = 12$, and found that the partial wave expansion falls almost exactly as $1/l^3$ for l=10, 11, and 12. The coefficient was determined from the l=12 result, and used to sum the remainder of the partial wave expansion, and an error estimate made by carrying out the same procedure with a coefficient found from the l=10 and l=11 results. That error was typically 0.0001 a.u., and could easily be reduced by either including more partial waves or using a more sophisticated extrapolation procedure. $E^{(0\text{-}P)}$, $E^{(1\text{-}P)}$, the pole term $E^{\rm pole}$, and the partial wave expansion of the modified main term are presented for lithiumlike uranium in Table I.

We now turn to a discussion of vacuum polarization. Because this is dominated by the Uehling potential, we incorporate screening in this potential only, leaving the screening corrections to the higher-order terms of the Wichmann Kroll expression for a later work. The Uehling potential for a distributed charge density $\rho(x)$ is

$$U(r) = -\frac{\alpha^2}{3\pi}\int_0^\infty dt(t^2-1)^{1/2}\left(\frac{2}{t^2}+\frac{1}{t^4}\right) \times \int d^3x\rho(x)\frac{e^{-2mt|\mathbf{r}-\mathbf{x}|}}{|\mathbf{r}-\mathbf{x}|}. \quad (15)$$

We evaluate this with an adaptive Gaussian integration scheme. The charge density is taken to be the nuclear charge density alone for the one-electron case, and that density reduced by the electronic charge density of the core electrons for the core-Hartree case. As we found very good agreement for the finite-nuclear-size-case (FNS) with the tabulation in Ref. [10], only the core-Hartree Uehling potential results are given below.

V. RESULTS AND DISCUSSION

It is now a straightforward matter to calculate the Lamb shift in any local non-Coulomb potential desired. We will not present the point-Coulomb results here, as they have already been accurately determined in Refs. [3] and [18]. However, for each state considered here they were calculated and found to equal the known results to within the estimated numerical precision. We first present the self-energy results for the finite-nuclear-size case. In Table II the self-energy of the $1s_{1/2}$ state for this case is presented for $Z = 60$, 70, 80, and 90 and compared to the previous calculation of Johnson and Soff [10]. It is seen that the previous results are consistently too large by about 40%, which is presumably due to the numerical difficulties of the BLS method described above. An interpolating formula that is valid at under the 0.001 a.u. level for intermediate values is

$$\Delta E(\mathrm{SE})_{\rm FNS}(1s_{1/2}) = -(Z\,R_{\rm rms}/a_0)^{2\gamma}[986Z^3 + 0.064Z^5]\alpha^3/\pi \quad (16)$$

where $R_{\rm rms}$ is the root mean square radius tabulated in

TABLE II. Finite-nuclear-size corrections to the electron self-energies of the $1s_{1/2}$ states of hydrogenlike ions (in a.u.).

Z	Present calculation	Ref. [10]
60	−0.0030(1)	−0.0048(13)
70	−0.0107(1)	−0.0181(30)
80	−0.0366(2)	−0.0598(56)
90	−0.1249(2)	−0.1880(110)

TABLE III. Finite-nuclear-size corrections to the electron self-energies of the $2s_{1/2}$ states of hydrogenlike ions (in a.u.).

Z	Present calculation	Ref. [10]
60	−0.0004(1)	−0.0007(3)
70	−0.0017(1)	−0.0029(6)
80	−0.0065(2)	−0.0103(13)
90	−0.0239(4)	−0.0343(30)

Ref. [10] and $\gamma = \sqrt{1-(Z\alpha)^2}$. In Table III the same calculation is presented for the $2s_{1/2}$ state. In this case the results of Ref. [10] are again seen to be about 40% too large. It is possible to interpolate intermediate values to an accuracy of 0.001 a.u. by using

$$\Delta E(\mathrm{SE})_{\mathrm{FNS}}(2s_{1/2})$$

$$= -(Z\ R_{\mathrm{rms}}/a_0)^{2\gamma}[84.9Z^3 + 0.025Z^5]\alpha^3/\pi. \quad (17)$$

In Table IV the self-energy for the $2p_{1/2}$ state is presented. In this case the overestimate of Ref. [10] is about a factor of 2.5, and an interpolating formula good to 0.0001 a.u. is

$$\Delta E(\mathrm{SE})_{\mathrm{FNS}}(2p_{1/2})$$

$$= (Z\ R_{\mathrm{rms}}/a_0)^{2\gamma}(Z\alpha)^2[11.6Z^3 - 0.008Z^5]\alpha^3/\pi. \quad (18)$$

The finite-nuclear-size effect for $2p_{3/2}$ states was found to be entirely negligible and is not tabulated here. We note in passing that in Ref. [19] we estimated the finite-nuclear-size effect for the $2p_{1/2}$-$2s_{1/2}$ splitting in uranium to be 0.6 eV. Although not explicitly quoted, an error of 0.2 eV was associated with this calculation. With the present more accurate method and a Fermi distribution with c =7.140 fm, a=0.523 fm, we now obtain a splitting of 0.794(4) eV, which is consistent with the results of Ref. [22] and a recent calculation of Mohr and Soff [26].

Tables V and VI present the core-Hartree results for the electron self-energy and Uehling potential part of vacuum polarization, respectively, appropriate for the lithiumlike isoelectronic system. Recently a rather complete calculation of these results has been made by Blundell [27]: the present calculation is in excellent agreement with his. However, the only experimental result in this range is the measurement of the $2p_{1/2}$-$2s_{1/2}$ splitting in lithiumlike uranium [28], which was found to be 280.59(10) eV. Our present result for the contribution to this splitting from the sum of the self-energy and Uehling potential part of vacuum polarization given in Table I is −1.5054(6) a.u., and is consistent with, but more accurate than, our previous result [19] −1.504(3) a.u. We note that while this result is in agreement with Refs. [22] and [23], a discrepancy with the calculation of Indelicato and Mohr [29] remains to be explained. However, the theoretical situation has changed slightly because of a sign error made in Ref. [30] in the nuclear polarization contribution. This contribution to the $2p_{1/2}$-$2s_{1/2}$ splitting was given as −0.126 eV, when it should have been +0.126 eV. The magnitude of this number was obtained by scaling the $1s_{1/2}$ calculation presented in Ref. [31]: however, the calculation for the n =2 states was later carried out explicitly in Ref. [17], and the direct calculation gives 0.18(5) eV. This changes the non-QED contribution to 322.55(6) eV, which leads to an experimentally inferred QED effect of −41.96(12) eV. Adding the self-energy and Uehling potential results from Table I to the Wichmann-Kroll, higher-order, and relativistic recoil corrections of −0.024(5) a.u. obtained from Ref. [10], the theoretical QED effect calculated here is −41.58(14) eV, which leaves a 0.38(18)-eV discrepancy. However, as emphasized in the introduction, the QED parts of the graphs of Fig. 2 remain to be calculated. While certain sets of these graphs have been considered [27, 29], until a complete calculation has been carried out, one can only observe that evaluation of the Lamb shift in the core-Hartree potential accounts for the bulk of the experimentally inferred QED effect.

In conclusion, we have presented in this paper a set of one-loop Lamb-shift calculations in non-Coulomb potentials. Higher accuracy than possible with the BLS method has been achieved by adopting the improvements of Refs. [21] and [22]. Even though entirely different nu-

TABLE IV. Finite-nuclear-size corrections to the electron self-energies of the $2p_{1/2}$ states of hydrogenlike ions (in a.u.).

Z	Present calculation	Ref. [10]
60	−0.000 01	−0.000 02
70	−0.000 06	−0.000 15
80	−0.000 36(1)	−0.000 95
90	−0.001 93(4)	−0.004 67(10)

TABLE V. Core-Hartree self-energy for n = 2 states of Li-like ions (in a.u.).

Z	$2s_{1/2}$	$2p_{1/2}$	$2p_{3/2}$
60	0.3952(5)	0.0078(5)	0.0386(5)
70	0.7180(5)	0.0351(5)	0.0807(5)
80	1.2402(5)	0.1040(5)	0.1534(5)
90	2.0801(5)	0.2641(5)	0.2703(5)

TABLE VI. Uehling potential part of core-Hartree vacuum polarization for n =2 states of Li-like ions (in a.u.).

Z	$2s_{1/2}$	$2p_{1/2}$	$2p_{3/2}$
60	−0.057 65	−0.003 18	−0.000 27
70	−0.123 29	−0.010 0 0	−0.000 73
80	−0.251 87	−0.028 7 4	−0.001 68
90	−0.504 15	−0.078 77	−0.003 49

merical methods are used, there is excellent agreement between the results of the two groups. Large discrepancies with a previous tabulation of finite-nuclear-size effects on the self-energy have been found, and the theoretical status of lithiumlike uranium updated. The 0.4(2)-eV discrepancy now present in that system presents an outstanding challenge to relativistic many-body theory, and the complete evaluation of the Feynman graphs of Fig. 2 is now a central problem for the physics of highly charged ions.

ACKNOWLEDGMENTS

We would like to thank Steve Blundell, Peter Mohr, and Neal Snyderman for helpful conversations. Some of the calculations were carried out on the NCSA CRAY Y-MP computer. The research of W. R. J. and J. S. was supported by NSF Grant No. PHY-90-12408. The work of K. T. C. was performed under the auspices of the U.S. Department of Energy by Lawrence Livermore National Laboratory under Contract No. W-7405-ENG-48.

[1] H.T. Doyle, *Advances in Atomic and Molecular Physics* (Academic, New York, 1969), Vol. 5, p. 337.
[2] W.R. Johnson, S.A. Blundell, and J. Sapirstein, Phys. Rev. A **37**, 2764 (1988); **38**, 2699 (1988); **42**, 1087 (1990).
[3] P.J. Mohr, At. Data Nucl. Data Tables **29**, 453 (1985).
[4] J.P. Desclaux, Phys. Scr. **21**, 436 (1980); P. Indelicato *et. al.*, J. Phys. B **20**, 651 (1987); P. Indelicato and J.P. Desclaux, Phys. Rev. A **42**, 5139 (1990).
[5] P.J. Mohr, Phys. Rev. A **32**, 1949 (1985).
[6] M. Gell-Mann and F. Low, Phys. Rev. **84**, 350 (1951).
[7] J. Sucher, Phys. Rev. **107**, 1448 (1957).
[8] W.H. Furry, Phys. Rev. **81**, 115 (1951).
[9] J. Sapirstein, Nucl. Instrum. Methods B **43**, 338 (1989).
[10] W.R. Johnson and G. Soff, At. Data. Nucl. Data Tables **33**, 405 (1985).
[11] An extensive set of references is given by Gerhard Soff and Peter J. Mohr, Phys. Rev. A **38**, 5066 (1988).
[12] See the discussion in J. Sapirstein and D.R. Yennie, in *Quantum Electrodynamics*, edited by T. Kinoshita (World Scientific, Singapore, 1990).
[13] G.E. Brown, J.S. Langer, and G.W. Schaefer, Proc. R. Soc. London Ser. A **251**, 92 (1959).
[14] G.E. Brown and D.F. Mayers, Proc. R. Soc. London Ser. A **251**, 92 (1951).
[15] A.M. Desiderio and W.R. Johnson, Phys. Rev. A **3**, 1267 (1971).
[16] K.T. Cheng and W.R. Johnson, Phys. Rev. A **14**, 1943 (1976).
[17] Günter Plunien, Berndt Müller, Walter Greiner, and Gerhard Soff, Phys. Rev. A **43**, 5853 (1991).
[18] Yong-Ki Kim and P.J. Mohr, Phys. Rev. A **1**, 123 (1991).
[19] K.T. Cheng, W.R. Johnson, and J. Sapirstein, Phys. Rev. Lett. **66**, 2960 (1991).
[20] Neal J. Snyderman, Ann. Phys. (N.Y.) **211**, 43 (1991).
[21] S.A. Blundell and N. Snyderman, Phys. Rev. A **44**, R1427, 1991.
[22] S.A. Blundell, Phys. Rev. A **46**, 3762 (1992).
[23] H. Persson, I. Lindgren, and S. Salomonson, Phys. Scr. (to be published).
[24] I.P. Grant and H. Quiney, Phys. Scr. (to be published).
[25] G.P. Lepage, J. Comput. Phys. **27**, 192 (1978).
[26] P. Mohr and G. Soff, Phys. Rev. Lett. **70**, 158 (1993).
[27] S.A. Blundell, Phys. Rev. A **47**, 1790 (1993).
[28] J. Schweppe, A. Belkacem, L. Blumenfeld, Nelson Claytor, B. Feinberg, Harvey Gould, V.E. Kostroun, L. Levy, S. Mishawa, J.R. Mowat, and M. Prior, Phys. Rev. Lett. **66**, 1434 (1991).
[29] P. Indelicato and P.J. Mohr, Theor. Chem. Acta **80**, 207 (1991).
[30] S.A. Blundell, W.R. Johnson, and J. Sapirstein, Phys. Rev. A **41**, 1698 (1989).
[31] G. Plunien, B. Müller, W. Greiner, and G. Soff, Phys. Rev. A **39**, 5428 (1989).